

## Non-Linear Control of a DC Microgrid for Electric Vehicle Charging Stations

Abdelkarim Benamar<sup>a</sup>, Pierre Travailleur<sup>a\*</sup>, Jean-Michel Clairand<sup>b</sup>, Guillermo Escrivá-Escrivá<sup>c</sup>

<sup>a</sup>*Ecole Nationale Supérieure de l'Electronique et Ses Applications (ENSEA), 6 Avenue du Ponceau, Cergy, 95000, France  
E-mail: pierre.travailleur@ensea.fr, \*abdelkarim.benamar@ensea.fr*

<sup>b</sup>*Facultad de Ingeniería y Ciencias Agropecuarias, Universidad de las Américas- Ecuador, José Queri S/N, Quito, 170122, Ecuador  
E-mail: jean.clairand@udla.edu.ec*

<sup>c</sup>*Institute for Energy Engineering, Universitat Politècnica de València, Camino de Vera S/N, edificio 8E, escalera F, 3a planta, Valencia, 46022, Spain  
E-mail: guieses@die.upv.es*

---

**Abstract**— Environmental concerns push governments to invest in renewable energy (RE). They are natural sources with a low carbon footprint and do not pollute locally. However, it is technically difficult to deploy high penetration of RE into the utility grid, due to the generation uncertainties and high installation costs, which are some of the most critical issues in RES use in this area. To address this issue, DC microgrids arise as a solution to integrate local distributed generation (DG) and storage, and to mitigate the issues related to AC/DC and DC/AC converters. Thanks to their main advantages for the power grid and energy consumers, microgrids have gained significant interest in recent years. By another side, the electric vehicles (EVs) market is expected to grow in the coming years, which represent a new load that must be properly managed to avoid grid issues. Thus, this paper discusses the operation of DC microgrid considering the introduction of EVs. A nonlinear control is presented, including the modeling of charging of EVs. The simulated DC microgrid includes solar PV, a battery, and a supercapacitor. Significant variations from PV generation were included to highlight the performance of the methodology. The results show that the voltage fluctuations are small, which provides the DC microgrid with the required voltage stability. Moreover, it has been demonstrated that DC microgrids can be integrated in isolated locations that are not connected to the main grid in view of the RESs and EVs.

**Keywords**— electric vehicle; smart grid; DC microgrid; nonlinear control.

---

### I. INTRODUCTION

Microgrids have gained important attention last year because of their main advantages for the power grid and the electricity customers. The advantages include power quality improvement, emissions reduction, network congestion and power loss reduction, and energy efficiency increase [1].

The idea of microgrid was to aggregate micro sources and loads into one unique entity, which could be interpreted as a single dispatchable prosumer from the overhead power system viewpoint [2]. A microgrid is defined as a cluster of loads, distributed generation (DG) units and energy storage systems (ESSs) operated in coordination to reliably supply electricity, connected to the host power system at the distribution level at a single point of connection, the Point of Common Coupling (PCC) [3]. Furthermore, microgrids can operate autonomously or be grid-connected, and depends on the type of voltage: AC, DC, or hybrid [4].

Microgrids generally integrate renewable based distributed generation (DG) units and energy storage systems (ESSs). Some of the DG units are wind turbines, photovoltaic (PV) panels, fuel cells, and microturbines, while ESSs are batteries, flywheels, and supercapacitors [5]. These are the key components of the microgrids, and they are considered as the main solution for remote communities without access to a main grid.

Several research has been performed in AC microgrids, but in recent years DC microgrids have attracted significant attention due to higher efficiency, better performance for many types of renewable energy sources (RESs) and ESS, and better compliance with DC consumer electronics, among others [6], [7]. Moreover, when components are coupled around a DC bus, there are no issues with reactive power flow, power quality, and frequency regulation [8], resulting in a notably less complex control system [4]. Nevertheless, some drawbacks have to be addressed while implementing DC microgrids, such as the need to build DC distribution

lines, the protection of DC systems is more difficult, and the loads adapted for DC power supply are required for high system efficiency [9].

Electric Vehicles (EVs) represent a proper solution to mitigate pollution problems and to achieve low-carbon transport transition. The deployment of EVs in RE-based microgrids results much more beneficial in terms of emissions, which have already been studied by researchers [10]–[12]. However, just a few works have considered the operation of DC microgrids considering the introduction of EVs, such as [13], [14]. EVs owns large capacity batteries, which must be charged with DC power. The typical charging consists on connecting to an AC network, where the AC power is converted to DC by an EV charger that includes an AC/DC converter. Therefore, EVs could result in a crucial DC load for DC microgrids.

The growing introduction of RESs as DG units introduce some challenges in the operation of in DC microgrids. One particular challenge is to ensure the voltage stability, which is defined as "the ability of a power system to maintain steady voltages at all buses in the system after being subjected to a disturbance from a given initial operating condition" [15]. The variations in the RES generation and uncertainties generate voltage drops and voltage stability issues. Hence, some researchers have proposed some methodologies to control voltage. For example, in [16], the autonomous DC voltage control for a DC microgrid with multiple power and slack terminals, which respond to the generation variation and load step, is proposed. The authors of [17] study the cooperative voltage control scheme of a large DC microgrid with a DG and a grid connected converter. In [18], an Input-to-State-Lyapunov based nonlinear control approach for DC microgrids is presented considering plug and play philosophy to enable efficient integration of RES.

These works and others have demonstrated their effectiveness; however, less attention has been devoted to nonlinear control of DC microgrids considering the introduction of new DC loads such as EVs, which is the aim of this paper. The case studio of Galápagos, Ecuador is considered, where real PV data is used and a fleet of EVs are considered.

The rest of the paper is organized as follows: Section II presents the modeling of the EV charging station. Section III discusses the Nonlinear control. Section IV presents the simulation results. Finally, Section V is devoted to the conclusions.

## II. MATERIALS AND METHOD

This section describes the DC microgrid configuration and the EV modeling.

### A. Microgrid configuration

The assumed microgrid is composed by a photo-voltaic (PV) panel, a battery, a supercapacitor and DC/DC converters, as depicted in Fig. 1. The battery and super capacitor allow avoiding disturbances during the transients. The battery provides a low frequency current and the super

capacitor provides a high frequency current. The DC/DC converter is a boost converter.

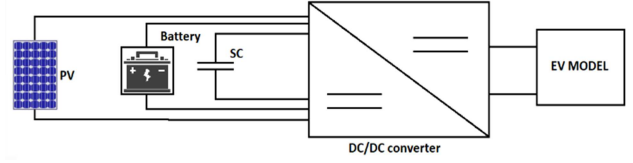


Fig. 1 EV charging station model.

The DC/DC Boost converter includes three phases, with six switches connected in parallel per phase, which are independently controlled with three different duty cycles. These duty cycles are used to control the power flow among PV, the batteries, and the EV.

All this source connected in parallel. With this configuration, the mathematical model is obtained based on power electronics averaging technique, as per [19], [20].

$$\frac{dV_{C1}}{dt} = \frac{V_{PV}}{R_1 C_1} - \frac{V_{C1}}{R_1 C_1} - \frac{I_{L1}}{C_1} \quad (1)$$

$$\frac{dV_{C2}}{dt} = \frac{V_{BAT}}{R_2 C_2} - \frac{V_{C2}}{R_2 C_2} - \frac{I_{L2}}{C_2} \quad (2)$$

$$\frac{dV_{C3}}{dt} = \frac{V_{SC}}{R_3 C_3} - \frac{V_{C3}}{R_3 C_3} - \frac{I_{L3}}{C_3} \quad (3)$$

$$\frac{dI_{L1}}{dt} = \frac{V_{C1}}{L_1} - \frac{[(R_{01}-R_{02})u_1+R_{02}]I_{L1}}{L_1} - \frac{(1-u_1)V_{DC}}{L_1} \quad (4)$$

$$\frac{dI_{L2}}{dt} = \frac{V_{C2}}{L_2} - \frac{[(R_{03}-R_{04})u_2+R_{04}]I_{L2}}{L_2} - \frac{(1-u_2)V_{DC}}{L_2} \quad (5)$$

$$\frac{dI_{L3}}{dt} = \frac{V_{C3}}{L_3} - \frac{[(R_{05}-R_{06})u_3+R_{06}]I_{L3}}{L_3} - \frac{(1-u_3)V_{DC}}{L_3} \quad (6)$$

$$\frac{dV_{DC}}{dt} = \frac{1}{C_{DC}} [(1-u_1)I_{L1} + I_{L2} + I_{L3} - I_{LOAD}] \quad (7)$$

$$I_{LOAD} = I_{L4} + I_{L5} + I_{L6} \quad (8)$$

Where  $V_{C1}$ ,  $V_{C2}$ , and  $V_{C3}$  are the voltages of capacitors  $C_1$ ,  $C_2$ , and  $C_3$ .  $V_{PV}$ ,  $V_{BAT}$ ,  $V_{SC}$ ,  $V_{DC}$  are the PV panel, battery, supercapacitor, and DC microgrid voltages.  $I_{L1}$ ,  $I_{L2}$ , and  $I_{L3}$  are the currents in the inductances  $L_1$ ,  $L_2$  and  $L_3$ . The resistors  $R_{01}$ ,  $R_{02}$ ,  $R_{03}$ ,  $R_{04}$ ,  $R_{05}$ , and  $R_{06}$  are the resistances of the switches of the converter.  $u_1$ ,  $u_2$ , and  $u_3$  are the duty cycle of the converters.  $I_{LOAD}$  is the current of the load.  $I_{L4}$ ,  $I_{L5}$ , and  $I_{L6}$  are the currents used for the EVs.

### B. EV modelling

The charger of the EV is modeled, as illustrated in Fig. 2. The total load considers three EVs connected in parallel. The assumed capacity of the EVs corresponds to a bus battery. The electronic model of the EV can be modeled by one battery, one resistance one capacitor and two switches.

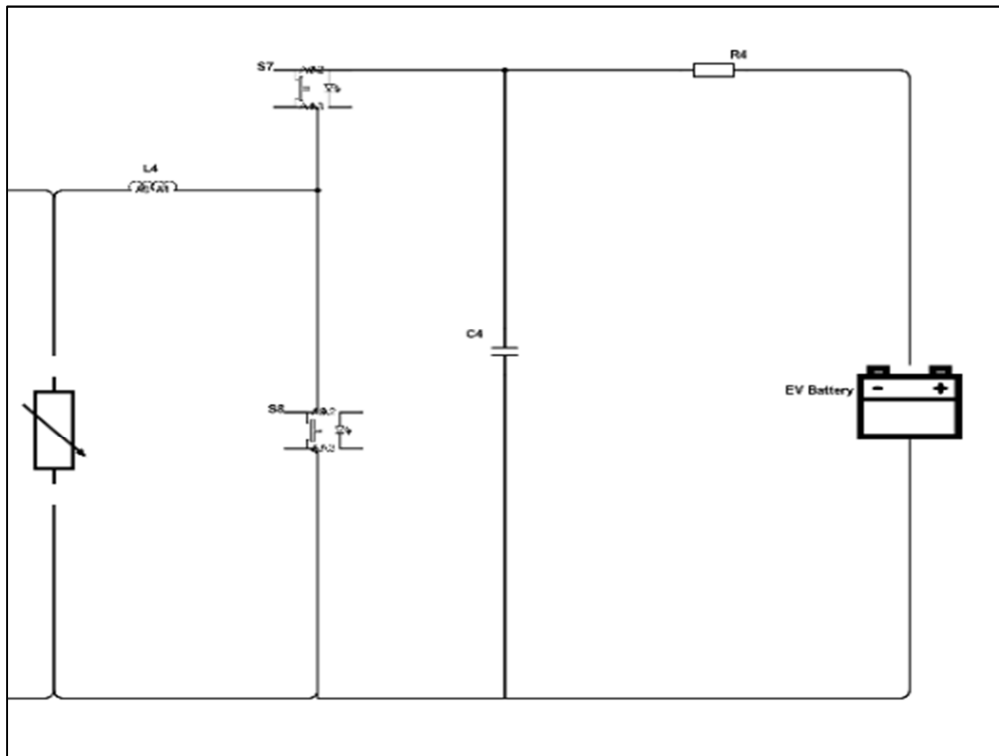


Fig. 2 EV model.

### C. Control of $V_{DC}$

As mentioned before, the DC microgrid can suffer stability issues due to the uncertainties of the PV generation and the load. Thus, a control system is required to remain the voltage in adequate levels, and to ensure the stability. A nonlinear control for the system is designed to manage the

voltage and current in the DC microgrid. The scheme of this control is represented in Fig. 3. The selection of nonlinear control was considered since this control is more performing than a simple PID control and the implementation in the software is not time demanding [20].

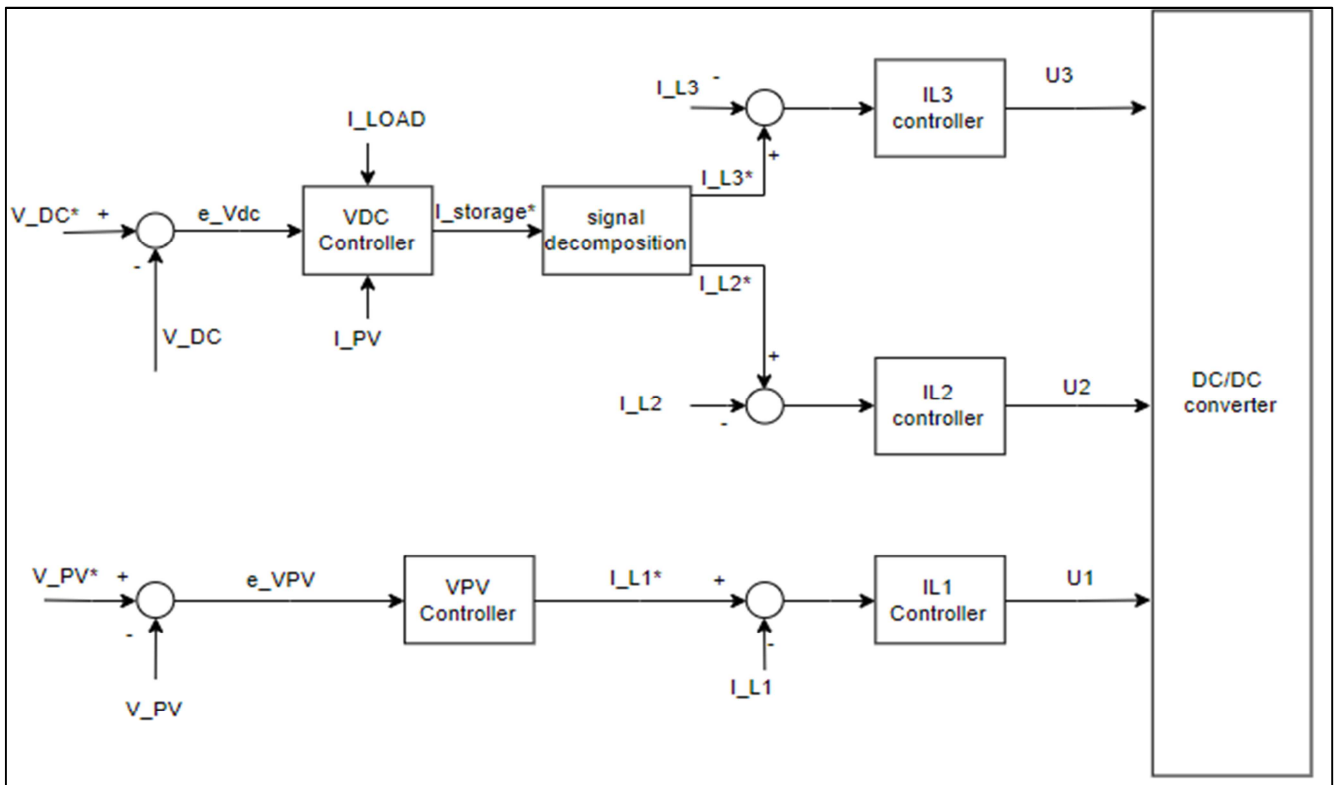


Fig. 3 Control Model.

To control the voltage  $V_{DC}$ , the error between  $V_{DC}$  and  $V_{DC}^*$ , which is its reference value, is calculated. The integrator of this error is also calculated.

$$e_{V_{DC}} = (V_{DC} - V_{DC}^*) \quad (9)$$

$$\dot{\alpha}_7 = K_7^\alpha e_{V_{DC}} \quad (10)$$

$$e_{V_{DC}} = K_7 e_{V_{DC}} - \bar{K}_7 \alpha_7 \quad (11)$$

From (7) and (11), it can be written:

$$(I_{L2} + I_{L3})^* = \frac{V_{DC}}{R_{LOAD}} - (1 - u_1)I_{L1} - \bar{K}_7 C_C \alpha_7 - K_7 C_{DC} (V_{DC} - V_{DC}^*) \quad (12)$$

with  $K_7$ ,  $\bar{K}_7$ , and  $K_7^\alpha$ , positive gains that are used to impose desired dynamics to the closed loop system. Then:

$$\begin{pmatrix} \dot{\alpha}_7 \\ e_{V_{DC}} \end{pmatrix} = \begin{pmatrix} 0 & K_7^\alpha \\ -\bar{K}_7 & K_7 \end{pmatrix} \begin{pmatrix} \alpha_7 \\ e_{V_{DC}} \end{pmatrix} \quad (13)$$

Thus, the eigenvalues are:

$$\lambda_{7.1} = -0.5 \left( K_7 + \sqrt{K_7^2 - 4\bar{K}_7 K_7^\alpha} \right) \quad (14)$$

$$\lambda_{7.2} = -0.5 \left( K_7 - \sqrt{K_7^2 - 4\bar{K}_7 K_7^\alpha} \right) \quad (15)$$

Through these eigenvalues the transfer function  $H_7$  can be written:

$$H_7 = \frac{1}{s^2 + K_7 s + K_7^\alpha \bar{K}_7} = \frac{G}{\omega_7^2 + 2\frac{\zeta}{\omega_7} s + 1} \quad (16)$$

With  $G$  the gain of this transfer function,  $\omega_7$  the eigenpulsation, and  $\zeta$  a constant that helps to tune the dynamic. Thus:

$$\omega_7 = \sqrt{\bar{K}_7 K_7^\alpha} \zeta = \frac{K_7}{2\sqrt{\bar{K}_7 K_7^\alpha}} \quad (17)$$

For the dynamic, it was chosen  $\omega_7 = \frac{2\pi}{0.1} = 62.8 \text{ rad} \cdot \text{s}^{-1}$ ,

$$\zeta = \frac{\sqrt{2}}{2}, \text{ and } K_7^\alpha = 1$$

#### D. Current Control

Based on the first part of this control, it is possible to know the current needed in the system. The current  $(I_{L2} + I_{L3})^*$  was divided in low frequency and high frequency.  $I_{L2}$  is the low frequency current and  $I_{L3}$  is the current high frequency. This decomposition is supported by a low frequency filter.

1) *Control of  $I_{L2}$* : For the current control, it was used a same nonlinear control.

$$e_{I_{L2}} = (I_{L2} - I_{L2}^*) \quad (18)$$

$$\dot{\alpha}_4 = K_4^\alpha e_{I_{L2}} \quad (19)$$

$$e_{I_{L2}} = K_4 e_{I_{L2}} - \bar{K}_4 \alpha_4 \quad (20)$$

With the equation (19) and (5) we can obtain:

$$u_2 = \frac{1}{(V_{DC} + (R_{04} - R_{03})I_{L2})} \cdot [V_{DC} - V_{C2} + R_{04}I_{L2} - L_2(K_4 e_{I_{L2}} + \bar{K}_4 \alpha_4 - I_{L2}^*)] \quad (21)$$

To tune the constant  $K_4$ ,  $\bar{K}_4$  and  $K_4^\alpha$ , it was used the same method in the previous part. Thus  $K_4 = 8796$ ,  $\bar{K}_4 = 6283^2$  and  $K_4^\alpha = 1$ .

2) *Control of  $I_{L3}$* : With the previous method, the equation is:

$$u_3 = \frac{1}{(V_{DC} + (R_{06} - R_{05})I_{L2})} \cdot [V_{DC} - V_{C3} + R_{06}I_{L3} - L_3(K_6 e_{I_{L3}} + \bar{K}_6 \alpha_6 - I_{L3}^*)] \quad (22)$$

For the choice of the constants, it was chosen:

$$\begin{aligned} K_6 &= 1 \\ \omega_6 &= 2 \cdot \pi \cdot 10\,000 \\ \zeta_6 &= \frac{\sqrt{2}}{2} \end{aligned}$$

#### E. Control of $V_{PV}$ and $I_{L1}$

The last part of this control corresponds to the PV panel. Here the control uses two errors to manage the PV panel. The control considers the following equations, as per [20], [21]:

$$e_{V_{C1}} = (V_{C1} - V_{C1}^*) \quad (23)$$

$$e_{I_{L1}} = (I_{L1} - I_{L1}^*) \quad (24)$$

$$\dot{\alpha}_1 = K_1^* e_{V_{C1}} \quad (25)$$

$$\dot{\alpha}_2 = K_2^* e_{I_{L1}} \quad (26)$$

$$e_{V_{C1}} = -K_1 e_{V_{C1}} - \bar{K}_1 \alpha_1 \quad (27)$$

$$e_{I_{L1}} = -K_2 e_{I_{L1}} - \bar{K}_2 \alpha_2 \quad (28)$$

Where  $K_1$ ,  $\bar{K}_1$ , and  $K_1^\alpha$  are constants which allow modifying the dynamic of PV panel control. Using equations (1) and (22), it obtains:

$$I_{L1}^* = \frac{V_{PV} - V_{C1} + R_{02}I_{L1}}{V_{DC} + (R_{02} - R_{01})I_{L1}} \left[ L_1 - K_2(I_{L1} - I_{L1}^*) + \bar{K}_2 \alpha_2 - C_{1\bar{K}_1} K_1^* e_{V_{C1}} + \left( C_1 K_1 - \frac{1}{R_1} \right) (K_1 e_{V_{C1}} + \bar{K}_1 \alpha_1) \right]$$

and with (4) and (23), it obtains:

$$u_1 = \frac{1}{V_{DC} + (R_{02} - R_{01})I_{L1}} \cdot V_{DC} - V_{C1} + R_{02}I_{L1} \left[ L_1 - K_2(I_{L1} - I_{L1}^*) + \bar{K}_2 \alpha_2 - C_{1\bar{K}_1} K_1^* e_{V_{C1}} + \left( C_1 K_1 - \frac{1}{R_1} \right) (K_1 e_{V_{C1}} + \bar{K}_1 \alpha_1) \right] \quad (29)$$

### F. EV charging Control

It was assumed to charge the EVs with the maximum power of the microgrid. The equations for the control of the EVs are the following:

$$e_{I_{Li}} = (I_{Li} - I_{Li}^*) \quad (30)$$

$$\alpha_{charge_i} = K_{charge_i}^\alpha e_{I_{Li}} \quad (31)$$

$$e_{I_{Li}} = K_{charge_i} e_{I_{Li}} - \bar{K}_{charge_i} \alpha_{charge_i} \quad (32)$$

Where  $i \in [4, 5, 6]$ ,  $K_{charge_i}$ ,  $\bar{K}_{charge_i}$ , and  $K_{charge_i}^\alpha$  are dynamic constants.

The current  $I_{Li}^*$  is chosen to deliver maximum power. To calculate the duty cycle, it was used equation (31) and the topology of the EV circuit.

$$u_4 = \frac{1}{(V_{C4} + (R_{08} - R_{07})I_{L4})} \cdot (V_{C4} - V_{DC} + R_{08}I_{L4} - L_4(K_{charge_1} e_{I_{L4}} + \bar{K}_{charge_1} \alpha_{charge_1} - I_{L4}^*)) \quad (34)$$

$$u_5 = \frac{1}{(V_{C5} + (R_{010} - R_{09})I_{L5})} \cdot (V_{C5} - V_{DC} + R_{09}I_{L5} - L_5(K_{charge_2} e_{I_{L5}} + \bar{K}_{charge_2} \alpha_{charge_2} - I_{L5}^*)) \quad (35)$$

$$u_6 = \frac{1}{(V_{C6} + (R_{012} - R_{011})I_{L6})} \cdot (V_{C6} - V_{DC} + R_{012}I_{L6} - L_6(K_{charge_3} e_{I_{L6}} + \bar{K}_{charge_3} \alpha_{charge_3} - I_{L6}^*)) \quad (36)$$

Where  $u_4$ ,  $u_5$ , and  $u_6$  are duty cycles of converter of EV.

### III. RESULTS AND DISCUSSION

To demonstrate the effectiveness of the methodology, a case study was simulated. The software Simulink from MathWorks was used [22]. As previously mentioned, the microgrid is composed of a solar PV, a battery, and a supercapacitor, where the load of EVs is included. Real-data of solar PV from Santa Cruz, Galapagos Islands, Ecuador, is used. The data of September 10<sup>th</sup> 2014 between 10:20 and 10:50 was considered since the variations of the PV power are very high. Note that the interest of this control is that the DC microgrid needs to remain stable even with high variations of generation sources. The PV power profile is depicted in Fig. 4.

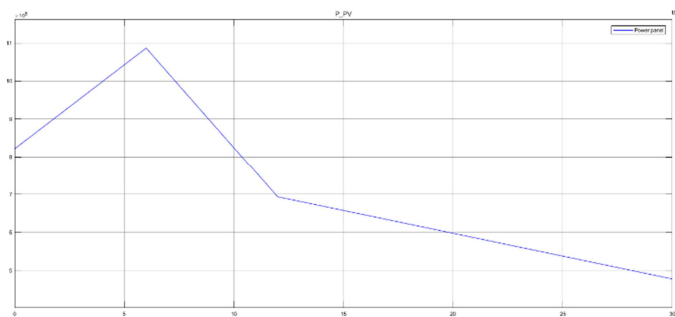


Fig. 4 PV power profile on September 10<sup>th</sup> 2014.

The simulation was performed in a horizon of 30 seconds, due to calculation limitations. This time horizon is

appropriate to observe the stability of the system during high variations of power generation.

Due to calculation limitations, the simulation was run in a period of 30 s. The variations remain similar. Consequently, the simulation has the same variation of power panel than Fig. 4, but on a shorter time.

The simulation follows the next steps:

- At second 1, the first electric bus is plugged on the microgrid with 95% power maximum that microgrid can provide.
- At second 9 another bus is plugged on the microgrid with 95% of power maximum that microgrid can provide, this power is divided by two equal shares.
- At second 12 the last bus is plugged with 95% of power maximum that microgrid can provide, this power is divided by three equal shares.
- At second 18 microgrid uses 100% of this power to recharge the buses.

The characteristics of the simulated electric bus are the ones of the BYD K9, with a charging power of 60 kW at 220 V, and with a battery capacity of 324 kWh [23]. The simulations are observed in Fig. 5 and Fig. 6. It is observed that the minimum voltage value is 396 V at second 9, which represents a variation of 1%, which is a low variation that will not generate stability issues. Moreover, the voltage returns in less than 100 ms to its reference value. The results demonstrate that the proposed methodology is effective for including EV charging in a DC microgrid.

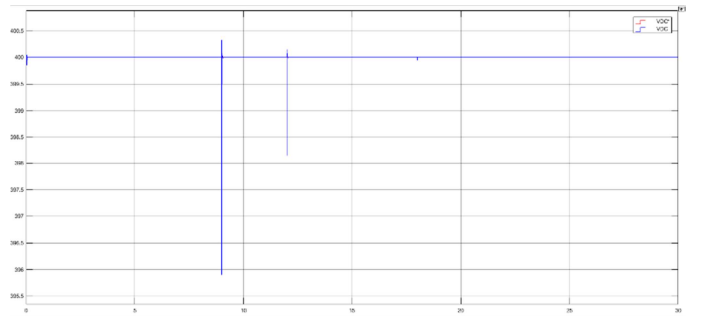


Fig. 5 Voltage pattern of DC microgrid during the simulation.

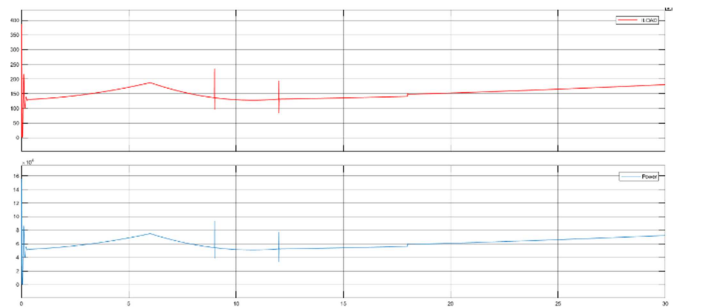


Fig. 6 Current and power used by the load during the simulation.

### IV. CONCLUSION

This paper presents the operation of a DC Microgrid considering the introduction of EVs. The studied DC Microgrid includes PV generation, a battery, and a supercapacitor. The EV load was also modeled. A nonlinear control is presented, which enables ensuring the voltage stability considering the fluctuations of the PV generation and of the EV load. The results indicate that the variations

of the voltage are minimal providing a proper voltage stability to the DC microgrid. In addition, it was shown that is possible to integrate DC microgrids considering RESs and EVs in isolated places, which are not connected to a main grid.

#### ACKNOWLEDGMENT

This work belongs to the project SIS.JCG.19.03 from Universidad de las Américas – Ecuador.

#### REFERENCES

- [1] H. Lotfi and A. Khodaei, "AC versus DC microgrid planning," *IEEE Trans. Smart Grid*, vol. 8, no. 1, pp. 296–304, 2017.
- [2] T. Dragičević, X. Lu, J. C. Vasquez, and J. M. Guerrero, "DC Microgrids - Part II: A Review of Power Architectures, Applications, and Standardization Issues," *IEEE Trans. Power Electron.*, vol. 31, no. 5, pp. 3528–3549, 2016.
- [3] D. E. Olivares *et al.*, "Trends in microgrid control," *IEEE Trans. Smart Grid*, vol. 5, no. 4, pp. 1905–1919, 2014.
- [4] T. Dragicevic, X. Lu, J. C. Vasquez, and J. M. Guerrero, "DC Microgrids - Part I: A Review of Control Strategies and Stabilization Techniques," *IEEE Trans. Power Electron.*, vol. 31, no. 7, pp. 4876–4891, 2016.
- [5] J. J. Justo, F. Mwasilu, J. Lee, and J. W. Jung, "AC-microgrids versus DC-microgrids with distributed energy resources: A review," *Renew. Sustain. Energy Rev.*, vol. 24, pp. 387–405, 2013.
- [6] B. Liu, F. Zhuo, Y. Zhu, and H. Yi, "System Operation and Energy Management of a Renewable Energy-Based DC Micro-Grid for High Penetration Depth Application," *IEEE Trans. Smart Grid*, vol. 6, no. 3, pp. 1147–1155, 2015.
- [7] P. Sanjeev, N. P. Padhy, and P. Agarwal, "Peak energy management using renewable integrated DC microgrid," *IEEE Trans. Smart Grid*, vol. 9, no. 5, pp. 4906–4917, 2018.
- [8] K. Liu, T. Liu, Z. Tang, and D. J. Hill, "Distributed MPC-Based Frequency Control in Networked Microgrids with Voltage Constraints," *IEEE Trans. Smart Grid*, vol. PP, no. c, pp. 1–1, 2019.
- [9] H. Kakigano, Y. Miura, R. Uchida, and I. Engineering, "Low-Voltage Bipolar-Type DC Microgrid for Super High Quality Distribution," *IEEE Trans. Power Electron.*, vol. 25, no. 12, pp. 3148–3154, 2010.
- [10] F. Locment and M. Sechilariu, "Modeling and simulation of DC microgrids for electric vehicle charging stations," *Energies*, vol. 8, no. 5, pp. 4335–4356, 2015.
- [11] K. W. Hu and C. M. Liaw, "Incorporated operation control of DC microgrid and electric vehicle," *IEEE Trans. Ind. Electron.*, vol. 63, no. 1, pp. 202–215, 2016.
- [12] J.-M. Clairand, J. Rodríguez-García, and C. Álvarez-Bel, "Electric Vehicle Charging Strategy for Isolated Systems with High Penetration of Renewable Generation," *Energies*, vol. 11, no. 11, pp. 1–21, 2018.
- [13] B. Aluisio, M. Dicorato, I. Ferrini, G. Forte, R. Sbrizzai, and M. Trovato, "Optimal sizing procedure for electric vehicle supply infrastructure based on DC microgrid with station commitment," *Energies*, vol. 12, no. 10, 2019.
- [14] M. I. Ghiasi, M. A. Golkar, and A. Hajizadeh, "Lyapunov Based-Distributed Fuzzy-Sliding Mode Control for Building Integrated-DC Microgrid with Plug-In Electric Vehicle," *IEEE Access*, vol. 5, pp. 7746–7752, 2017.
- [15] P. Kundur *et al.*, "Definition and Classification of Power System Stability," *IEEE Trans. Power Syst.*, vol. 19, no. 2, pp. 1387–1401, 2004.
- [16] D. Chen and L. Xu, "Autonomous DC voltage control of a DC microgrid with multiple slack terminals," *IEEE Trans. Power Syst.*, vol. 27, no. 4, pp. 1897–1905, 2012.
- [17] J. C. Choi, H. Y. Jeong, J. Y. Choi, D. J. Won, S. J. Ahn, and S. il Moon, "Voltage control scheme with distributed generation and grid connected converter in a DC microgrid," *Energies*, vol. 7, no. 10, pp. 6477–6491, 2014.
- [18] A. Iovine, M. Jim, and G. Damm, "Nonlinear Control for DC MicroGrids Enabling Efficient Renewable Power Integration and Ancillary Services for AC grids," *IEEE Trans. Power Syst.*, vol. 8950, no. c, pp. 1–10, 2018.
- [19] S. R. Sanders, J. M. Noworolski, X. Z. Liu, and G. C. Verghese, "Generalized Averaging Method for Power," *IEEE Trans. Power Electron.*, vol. 6, no. 2, pp. 251–259, 1991.
- [20] S. B. Siad, A. Malkawi, G. Damm, L. Lopes, and L. G. Dol, "Nonlinear control of a DC MicroGrid for the integration of distributed generation based on different time scales," *Int. J. Electr. Power Energy Syst.*, vol. 111, no. April, pp. 93–100, 2019.
- [21] A. Iovine *et al.*, "Voltage Stabilization in a DC MicroGrid by an ISS-like Lyapunov Function implementing Droop Control," *2018 Eur. Control Conf.*, pp. 1130–1135, 2018.
- [22] Mathworks, "Simulink." [Online]. Available: <https://es.mathworks.com/products/simulink.html>.
- [23] BYD, "Bus eléctrico K9G." [Online]. Available: <https://bydelectrico.com/buses-electricos/bus-electrico-k9/>.